On Gravity from SST, Geoid from SEASAT, and Plate Age and Fracture Zones in the Pacific

by

B. D. Marsh

Earth and Planetary Sciences

Johns Hopkins University

Baltimore, MD 21218

J. G. Marsh

Geodynamics Branch

Goddard Space Flight Center

Greenbelt, MD 20771

R. G. Williamson

EG&G Wash. Analytical Ser. Center Inc.

Riverdale, MD 20737

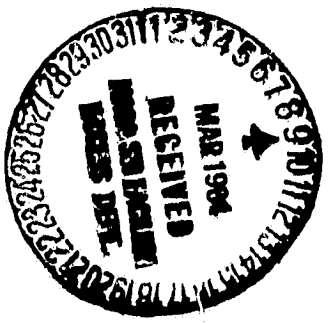

Abstract

Our earlier measurements of the high degree and order (n,m>12) gravity in the central Pacific using the method of satellite-to-satellite tracking (SST) have been extended with an additional 50 passes of data. The SST method utilizes line of sight Doppler tracking between the very high geosynchronous ATS-6 spacecraft and the much lower (840 km) orbiting GEOS-3 spacecraft. The observed changes in velocity with time are reduced relative to the well-determined low degree and order (n,m≤12) GEM-10 field model and accelerations are found by analytical differentiation of the range rates. This new map is essentially identical to the first map and we have produced a composite map by combining all 90 passes of SST data. The resolution of the map is at worst about 5° and much better in most places. A comparison of this map with conventional GEM models shows very good agreement. A reduction of the SEASAT altimeter data has also been carried out for an additional comparison. Although the SEASAT geoid contains much more high frequency information, it agrees very well with both the SST and GEM fields. The maps are dominated (especially in the east) by a pattern of roughly east-west anomalies with a transverse wavelength of about 2000 km. A further comparison with regional bathymetric data shows a remarkably close correlation with plate age. Each anomaly band is framed by those major fracture zones having large offsets and the regular spacing (≈10°) of these fractures seems to account for the fabric in the gravity field. There are other anomalies that are accounted for by hot spots and altogether the immediate

source of at least part of these Pacific anomalies is in the lithosphere itself. It therefore seems that most of the anomalies in the east half of the Pacific could be partly caused simply by regional differences in plate age. The amplitude of these geoid or gravity anomalies caused by age differences should decrease with absolute plate age, and large anomalies (~3 m) over old, smooth sea floor may indicate a further deeper source within or perhaps below the lithosphere. We have also considered the possible plume size and ascent velocity necessary to supply deep mantle material to the upper mantle without complete thermal equilibration. A plume emanating from a buoyant layer 100 km thick and 10^4 times less viscous than the surrounding mantle will have a diameter of about 400 km. And it must ascend at about 10 cm/yr to arrive still anomalously hot in the uppermost mantle.

Introduction

In an earlier paper we used the method pioneered by W. L. Sjogren of satellite-to-satellite tracking (SST) to measure the gravity field over the Pacific (Marsh et al., 1981). That study used 40 passes of ATS-6/GEOS-3 data to construct a high degree and order ($n,m > 12$) gravity map. The present study includes data from about 50 additional passes to produce a more detailed gravity map.

In brief, this method measures the earth's gravity field by Doppler tracking of a low orbiting satellite (GEOS-3 at 840 km) by a much higher (40,000 km) geosynchronous satellite (ATS-6). Doppler tracking furnishes the speed of the low satellite as a function of time or position. These range-rates are then converted through differentiation to line-of-sight accelerations or gravity anomalies. Point values of these anomalies measured along each track are then contoured into a map of gravity anomalies. The long wavelength components of the SST measurements are removed using a low degree and order ($n,m \leq 12$) field model, which is very well determined. The residual anomalies thus represent harmonics of $n,m > 12$.

The great advantage of the SST method is that it is simple. No large arrays of spherical harmonics need be found or manipulated, and there is little chance for the data to become numerically adulterated during processing. The method is limited by the height of the low-orbiting satellite and thus is sensitive to wavelengths longer than about 1500 km (i.e. $n,m \leq \approx 24$). But as shall be shown, it is this range of the gravity field ($12 \leq n,m \leq 25$) that is geophysically particularly interesting. A disadvantage of the method is that the map applies only at the altitude of 840 km and must be separately downward-continued to give anomalies on the earth's surface. This method also does not strictly measure the radial component of gravity, but rather

a changing line-of-sight component of the field between ATS-6 and GEOS-3. Only within 30-40 degrees of the high satellite's subsatellite point can these anomalies be taken as good measures of the radial field. Even with these limitations we found in our previous study that with only 15 passes of data the map derived of the gravity field over North America is essentially identical to that produced by any previous field model, which involves data from 30 or more satellites in addition to surface data.

The gravity data is not only geophysically useful, but it provides an excellent opportunity to check one gravity field against another. For example, in our previous study we compared the more conventional Goddard Earth Model (GEM10B; Lerch et al., 1981) and the SST gravity fields. We also show for the first time comparisons with the SEASAT altimeter-derived geoid over the Pacific, which is highly accurate and useful for comparisons and geophysical interpretations. We also show that there is often a good correlation between relatively young sea floor and gravity and geoid anomalies, the major fracture zones of the Pacific, because of their offsets, give the distinctive east-west fabric to the gravity and geoid anomalies. Other anomalies correlate with the traces of hot spots, and overall it is the interference of these two sources of anomalies that gives rise to the distinctive gravity field of the Pacific area.

SST Map

A map of satellite tracks used here and in our previous study are shown combined as Figure 1. The coverage is particularly dense over the central Pacific. The gravity is determined at 70 km intervals along each track and these values have been contoured into a map shown as Figure 2. This map shows the same assemblage of anomalies as we previously noted, but now there is more detail. In particular: The positive Line Islands anomaly, in the vicinity of the subsatellite point, is more rectangular and strikes nearly east-west. The positive tail on the southeast corner of this anomaly

is now smaller and essentially insignificant from zero. The positive anomaly around Hawaii (see plotted islands) and northeast of Hawaii is much the same as before except the contours within the anomaly show more detail. There is also now a stronger bridge of positive values between the Cook-Austral and Pitcairn anomalies. Otherwise the map is essentially the same as the previous SST map of Marsh et al., (1981).

Comparison with SEASAT Geoid

Since the geometry of an essentially radial gravity field is the same as its geoid, we show for comparison with the SST map a geoid over the same area (Figure 3). This geoid (mean sea surface) was computed using the radar altimeter from the SEASAT satellite and it represents 70 days of data taken between July and October 1978. The long wavelength field has again been removed by subtracting a low degree and order ($n,m \leq 12$) field model (PGS-S4; Lerch et al., 1982) from the original data. Each data point used in constructing this map represents an average of 1000 radar measurements taken over a time of 1 sec or a ground distance of 7 km, and each point has a precision of 3-4 cm (Tapley et al., 1982). The accuracy of the altimeter-derived mean sea surface with respect to the center of mass of the earth is dominated by radial orbit error. The recent SEASAT ephemerides computed at GSFC using laser and Unified S-Band tracking data and the most accurate earth gravity and geodetic models have a global rms radial accuracy of 70 cm. This set of data therefore contains far more high frequency information over the ocean than any previous GEM or SST gravity field. Through gridding and contouring, however, these data have been smoothed somewhat by using all points within a cap with a radius of five degrees. More details of the procedure of computing this mean sea surface are described by Marsh and Martin (1982).

Although the SEASAT geoid contains much more information than the SST map, the two maps show essentially the same anomalies. It should be recalled, however, that the relative zero-level between the two maps may be different and some features may appear larger or smaller on one or the other of the maps. There are nevertheless some significant differences. The Hawaiian anomalies (200°, 20°N; 215°, 30°N) are hardly connected on the SEASAT geoid. There is also a fairly strong geoid anomaly all along the chain of Hawaiian Islands. The SEASAT geoid shows almost a connection between the Hawaiian anomaly and the Line Islands anomaly to the south. Other than a small break near 190° the Line Island geoid anomaly nearly connects with the Gilbert-Marshall anomaly and forms a positive band nearly traversing the entire Pacific. On both maps this anomaly forms the backbone of the pattern of approximately east-west features with a transverse wavelength of about 2000 km. This had been seen in our earlier work but is now particularly clear in these maps.

In sum, the SST and SEASAT maps show the same basic areas of positive and negative anomalies and overall correlate closely. The SEASAT geoid provides a more complete coverage and over the Pacific as a whole is expected to be more accurate than the SST map.

Correlations with Fracture Zones and Hot Spot Traces

We noted in our recent (1981) paper that some of these gravity anomalies correlate well with residual depth anomalies. The Hawaiian and Cook-Austral anomalies, for example, correlate to various degrees with residual depth anomalies delineated by, respectively, Watts (1976) and Crough (1978).

And we found through a simple model that shallower-than-usual areas of the sea floor can certainly cause the requisite SST gravity anomaly if they are compensated at a depth of about 30-100 km. Some positive anomalies (e.g. northeast of Hawaii near 220° and 30°) apparently do not correlate with residual depth anomalies. The orderly pattern of east-west trending negative anomalies just south of Hawaii and the Line Islands anomalies, which nearly span the Pacific, apparently do not correlate with negative residual depth anomalies. Extensive residual depth data, however, is largely wanting.

Across fracture zones with large offsets in lithosphere age (≈10 m. y.) there is a significant change in thickness of the lithosphere, which is reflected by a sudden change in ocean depth. This step change in topography is well known to produce a distinctive gravity or geoid anomaly. The change with age of these anomalies has been used to study the aging and growth of the lithosphere (e.g. Detrick, 1981), and these anomalies may persist for great distances. In their study of the Mendocino fracture zone, for example, Sandwell and Schubert (1982) showed that these effects may persist to ages of 135 m.y., which corresponds to a distance near the bend in the Emperor-Hawaiian chain of seamounts. All of these studies, however, have used a local array of tracks to study a single anomaly or offset. Since the Pacific plate is cut by a regular pattern of fracture zones with large offsets, these may produce a certain fabric in the gravity and geoid fields.

To investigate such correlations between the gravity and geoid fields and regional bathymetry we first made a map of the 1° x 1° depths as

supplied by NOAA (1980) for the north Pacific. A comparison of Figure 2 and 3 with this map shows that major fracture zones essentially frame the east-west pattern of geoid and gravity anomalies. The major positive geoid anomaly northeast of Hawaii correlates with the relatively young lithosphere bounded between the Murray and Molokai fracture zones. Because the ocean floor magnetic anomalies closely record the age of the plate and thus also its bathymetry, there should also be a positive correlation between geoid anomalies and the age of the ocean basin as deduced from the magnetic anomalies of the sea floor. The superposition of geoid on plate age is shown as Figure 4. From this combined map there is a clear correlation between the gravity anomalies and the age of the lithosphere. The large fracture zones form a frame work around the gravity anomalies.

These correlations suggest that gravity and geoid anomalies not associated with active volcanism (i.e. so-called hot spots), especially in the eastern Pacific, may result from differences in age of the sea floor. The particular pattern of fracture zones where major offsets occur at approximately equally-spaced intervals (≈1000 km) produces a fabric in the geoid that dominates the entire Pacific.

If it were not for the seamount chains, the gravity and geoid fields of the Pacific would appear as approximately east-west bands of alternating sign. The topography and associated geoid fields of seamount chains are superimposed on this regional plate fabric, which is set at the ridges. Although the so-called hot spot seamount chains form at some distance from the ridge, other chains (e.g. Line Islands) have apparently formed near the ridge (Watts et al., 1980). Thus the Pacific gravity

and geoid fields are principally the result of these two distinctive effects. But because the course of the Pacific plate for the 42 m.y. has not been parallel to the pattern of fracture zones, the two sets of anomalies interfere. Hence we turn to a more detailed examination of the principal gravity and geoid anomalies and their relation to fracture zones, plate age, and hot spot activity.

Hawaiian Anomaly: The Hawaiian chain of seamounts, for example, cuts across the region bounded by the Murray and Molokai fracture zones which otherwise would be a positive band of gravity, and also across the negative region to the north between the Mendocino and Murray fracture zones (see Figure 5). This may have the resultant effect of producing the relative low in the geoid along the Hawaiian seamounts near the Midway Islands. This could have important implications for understanding the correlation of residual depth anomalies and geoid anomalies.

We found in our earlier (1981) study that the present gravity and geoid fields show positive anomalies at the bend in the Hawaiian-Emperor seamount chain. We also suggested that this anomaly may be an obstacle to Crough's (1978) model of lithospheric thinning near Hawaii, through local reheating, followed by a monotonic decay with cooling of both topography and geoid anomaly. If this anomaly at the bend is actually a continuation of the main Hawaiian chain anomaly, then the orginal Hawaiian anomaly may take longer than expected to decay. The eastern portion of this anomaly correlates with the shallow sea floor of the Hess Rise (e.g. Nemoto and Kroenke, 1981) but the western portion does not. Following Crough's model, however, even an original irregularity in the sea floor should be erased by the reheating and buoyant rise of the lithosphere to a virtual age of about 25 m.y. It is therefore not clear whether it is the positive anomaly at

the bend or the necking of the Hawaiian anomaly near Midway that is anomalous. For this model this differentiation could be important.

Line Islands Anomaly: A similar interference occurs between the east-west trending, positive Line Islands geoid anomaly band (Marsh et al., 1981) south of Hawaii and the trend of the Line Islands themselves. Watts et al. (1980) show that the gravity over the Line Islands is consistent with their geologic age of about 97 m.y., implying that they formed at a ridge. The continuation to the southeast of the trend of the Line Islands, however, has been volcanically active in the last 1.3 m.y. (Duncan and McDougall, 1974). Residual depth anomalies have been computed for this area by Crough and Jarrard (1981), who found that this anomaly decays roughly as predicted for a hot-spot trace that includes the inconsistently older Line Islands. This may imply that the Line Islands have been reheated, perhaps as a result of the more recent volcanism of the Cross Trend Line or from much earlier, unnoticed,intrusive activity of the Marquesas Islands.

This residual depth anomaly, the Marquesas-Line Swell (Crough and Jarrard, 1981), strikes northwesterly but more northerly than that of the trace of Pacific plate motion for the last 40 m.y. The associated geoid anomaly shown by Crough and Jarrard was derived from the GEOS-3 geoid of Brace (1977) by subtracting a regional geoid described by a seventh degree polynomial. This geoid anomaly also shows a WNW trend, a trend which is not evident in the more precise SEASAT geoid of Figure 3 nor in the SST and GEM gravity fields, each of which have had a twelfth degree global field removed. The trend of these latter fields is markedly east-west which persists for about 4000 km. In fact, a principal 4 m anomaly of

Brace's at -10°, 220°, which Crough and Jarrard found to correlate closely with the Marquesas depth anomaly, is absent in the SEASAT data. This descrepancy was described in our earlier (1981) SST study and was attributed to the sparseness of GEOS-3 altimeter data in this region. The extensive SEASAT data confirms this interpretation.

The WNW trend associated with the Line Islands is evident on the northwest corner of this regional anomaly, but any correlation with the Marquesas-Line Swell itself is less clear. The choice of removal of the regional field is evidently crucial in producing a geoid anomaly that correlates with this residual depth anomaly.

Regardless of the age of the Line Islands, they do produce a geoid anomaly trending NW, which might be expected, on grounds of seamount frequency, to continue through to the Hawaiian anomaly. These anomalies nearly do connect, but they are separated by a distinctive regional negative anomaly that spans the entire Pacific. This negative band has its origin on the east between the Clipperton and Murray fracture zones, which together frame relatively older lithosphere. The anomaly does not carefully follow these bounds, which is probably due to interference with the geoid anomaly of the Line Islands, and it cuts across moderately shallow (<5000 m) sea floor near 20° and 170-180°.

Cook-Austral Anomaly: This gravity and geoid anomaly centered near -20°,205° correlates roughly with the residual depth anomaly computed here by Crough (1978). On close inspection, the principal part of the depth anomaly (≈800 m) is near -28°,215° and trends northwesterly, which correlates with a tail of the geoid anomaly to the southeast. The amplitude of this

part of the geoid anomaly is never more than 2 m, which is significantly less than might be expected judging from past correlations. The much more regional nature of the geoid and gravity anomalies may in part be due to the proximity of the Tonga-Kermadec trench and its associated outer rise. It is also clear in this region that there is no positive anomaly over the Manihiki Plateau, which is just northeast of Samoa.

Early radiometric dating of lavas of the Cook-Austral Islands showed a broad consistency with the hot spot hypothesis, but four of these islands were updated and three others had only dates of unlocated samples. Turner and Jarrard (1982) have recently reported ninety four additional dates that supply this missing information. The ages of this chain now appear to be altogether inconsistent with those predicted by a simple hot spot migration. They instead suggest that the results give stronger support to a "hot line" hypotheses, which may stretch from the Samoan chain through the Cook-Australs and on to Pitcairn Island. A "hot line" could relate these volcanisms, but there seems to be little evidence of it in the gravity or geoid of this area.

Pitcairn Anomaly: This anomaly is bounded on the east by the east Pacific rise and on the north and south by two fracture zones with large offsets. It does not form a continuous band westward to the Cook-Austral anomaly, but is bounded on the west by a shallow negative anomaly (see more below).

Marshall-Gilbert Anomaly: This diffuse positive anomaly at 0°,180° is separated by a distinct but shallow low from the Line Islands anomaly to the east. The sea floor in this region is not highly populated with

seamounts and is generally 5000-6000 m deep. The tectonic history of this region of the Pacific is not clear, but the distinctly linear, north-northwest trending facing edges of these anomalies (i.e. Gilbert-Marshall and Line Islands) may suggest the presence of NNW trending fracture zones or other plate fabric. Some confirmation of this comes from the correlations of magnetic anomalies in this region whose strike is normal to the strike of the inferred fracture zones (e.g. Pitman et al., 1974). The chain of islands made up of the Marshall and Gilbert Islands, although also striking in this (NNW) direction, does not have an associated distinctive geoid anomaly. This general positive anomaly may therefore be caused by a region of relatively young sea floor (see below).

Geoid and Gravity Anomalies Between Fracture Zones

The step-like change in geoid height across fracture zones separating plates of different ages has been used to study the aging of the lithosphere by Crough (1979), Detrick (1981), and Sandwell and Schubert (1982). The amplitude of these anomalies is proportional to the offset in age, and the history of the anomaly can be used to evaluate the cooling characteristics and growth of the lithosphere. These results suggest deviations beginning at ages as early as 20-40 m.y. from the model of the lithosphere as a thermal boundary layer (Sandwell and Schubert, 1982). When modeled instead by the cooling of a plate of constant thickness, as suggested by Parsons and Sclater (1977), the closest fit to the change in slope of the geoid anomaly with age is for a plate thickness of 125 km (Sandwell and Schubert, 1982).

Although in these studies the proper separation of the anomaly due to the fracture zone from the regional field is critical, in interpreting the

residual SEASAT geoid of Figure 3 this is much less critical. This is so because the principal cause of the anomalies bounded by fracture zones is the regional difference in plate age. Each section of plate between the major fracture zones is large enough (≈1000 km) to be constantly near isostatic equilibrium. And each section of plate is large enough such that it has a characteristic geoid anomaly that, for the most part, depends critically on the absolute age of the plate. These points have been treated in some detail by Haxby and Turcotte (1978), Turcotte and McAdoo (1979), and Sandwell and Schubert (1980). Under the assumption of isostatic equilibrium, the geoid or gravity anomaly can be calculated from knowledge of the local vertical distribution of density as long as the depth of compensation is much less than the wavelength of the nomaly itself. For the plate regions between major fracture zones, the anomaly wavelength is ≈1000 km. The geoid anomaly N(x,y) due to a density distribution $\rho(x,y,z)$ over a depth L is given by (e.g. Turcotte and McAdoo, 1979)

$$N = -\frac{2\pi G}{g}\int_0^L z\Delta\rho(x,y,z)\,dz \qquad (1)$$

where z is the vertical coordinate, g is gravity at the surface and G is the universal gravitational constant. The application of (1) here is only an approximation. To model the details of the anomaly near fracture zones themselves the more exact techniques of, say, Sandwell and Schubert (1982) can be employed. For the broad scale anomalies considered here, however, results gained from (1) and also empirical relations (see below) should suffice.

Once a function for ρ is known throughout L, it is routine to compute N. For the present consideration, it is convenient to choose L as the thickness of the lithosphere. Since the thermal regime of the lithosphere changes with time, any equation of state will of necessity also be a

function of time. The result is not especially sensitve to the equation of state or to the assumed thermal distribution for times less than about 50 m.y.

For a thermal model of the lithosphere based on a thermal boundary layer, the geoid height relative to the ocean ridges is (Turcotte and McAdoo, 1979)

$$N = -\frac{1.17G\rho_2\alpha(T_L-T_o)L^2}{g}\left[1+\frac{2\rho_L\alpha(T_L-T_o)}{\pi(\rho_L-\rho_w)}\right] \qquad (2)$$

where ρ_L is the mantle density at a depth L at the base of the lithosphere where the temperature is T_L, T_o is the surface temperature, α is the isothermal coefficent of thermal expansion, ρ_w is the density of sea water and g is gravitational acceleration of the surface. A corresponding expression for the plate model is given by Sandwell and Schubert (1980). It is clear from (2) that the geoid anomaly is directly proportional to L^2, the thickness of the lithosphere, which for the thermal boundary layer model is $L^2 = (2.32)^2Kt$, where K is thermal diffusivity and t is time. With this substitution, (2) shows that the geoid anomaly is linearly dependent on the absolute age (t) of the lithosphere. Here we are interested in the anomaly caused because of the relative difference in age (Δt) of adjacent regions of plate bounded by fracture zones with large offsets (i.e. tens or more of millions of years). This relative geoid anomaly (ΔN) is thus given by

$$\Delta N = -6.30\,\frac{GBK}{g}\left[1+\frac{2B}{\pi(\rho_L-\rho_w)}\right]\Delta t \qquad (3)$$

where $B = \rho_L\alpha(T_L-T_o)$. The last term in brackets is always of order one and

it is clear that $\Delta N = -6.52\ GBK\ \Delta t/g$, which for $\rho_L = 3.30\ g/cm^3$, $g = 980\ cm/s^2$, $T_L - T_o = 1250°C$, $\alpha = 3.3 \times 10^{-5}\ deg^{-1}$, and $K \approx 10^{-2}\ cm^2/s$, $|\Delta N| = 1.75$ m per 10 m.y. of offset. This time difference ($\Delta t = 10$ m.y.) is reasonable for many fracture zones and the anomaly is of the same order as those shown by Figure 3.

Although this result may apply when the lithosphere is young, an unattractive feature of it is the fact that the relative geoid anomaly is independent of the absolute age of the lithosphere itself. Whereas it has been shown by Sandwell and Schubert (1980) that the rate of change of the geoid anomaly across fracture zones decreases systematically with plate age. Of the analytical models, they found that the plate model matches the data better than the boundary layer model. But overall a good estimate of the geoid anomaly can be obtained from the observed anomaly decay. Their actual data on the decay of the slope of the geoid anomaly with age for the North Atlantic is of the form (see their Figure 4)

$$\frac{dN}{dt} = 2 \times 10^{-3}\ t - 0.2 \qquad (4)$$

where N is the geoid height in meters and t is age in millions of years. Integrating (4) and employing the condition that N(t=0) = 0 and subtracting two such formulas for adjacent regions of, respectively, age t_1 and t_2 gives a result for the relative geoid anomaly.

$$\Delta N = (t_1^2 - t_2^2) \times 10^{-3} - 0.2(t_1 - t_2) \qquad (5)$$

Beginning at a ridge with a relative offset of 10 m.y. gives an anomaly of 1.9 m, which decays to about 1 m when the older plate has an age of 60 m.y., and the anomaly vanishes at an age of about 100 m.y. (The actual sign of the anomaly depends on the relative plate age.) From this result it is clear that geoid anomalies related to regional changes in plate age will only be significant over plates having an absolute age of less than about 80 m.y. The largest anomalies will of course be closest to the ridge and they will have decayed to near nothing over 80 m.y. In the Pacific significant anomalies can only be expected approximately east of the longitude of Hawaii. Overall it is useful, however, to apply these results to the interpretation of the aerially large positive anomalies that lie near the east Pacific rise; namely, the anomaly northeast of Hawaii, the eastern end of the Line Islands anomaly, and the Pitcairn anomaly.

The positive anomaly northeast of Hawaii is bounded by the Murray and Molokai fracture zones. Across the fracture zones in this vicinity the average offset in age is about 18 m.y. (Pitman et at., 1974). This would produce an anomaly of about 3 m when the actual anomaly approaches 6 m. This is not necessarily a serious dissagreement, because the anomaly directly to the north, over the older Murray-Mendocino area, is also positive and the relative difference is about 3 m. Why this positive spills northward to the Mendocino fracture zone and beyond may be due to the proximity of North America. Nevertheless it seems that this relative 3 m anomaly decreases markedly toward Hawaii. This may be due in part to a change in the offset age as has been noted for the Mendocino fracture zone by Sandwell and Schubert (1982).

Moving south, the next section of plate with a major offset is bounded by the Molokai and Clipperton fracture zones. This plate is relatively older and the geoid anomaly is slightly negative. The next positive anomaly is immediately to the south and is bounded, although not tightly, by the Clipperton and Galapagos fracture zones. The anomaly itself seems too broad

to be wholly the result of this relatively small offset (≈5 m.y.), which would produce about 1 m anomaly when the actual anomaly has an average amplitude of about 2 m. The anomaly nearly reaches the Marquesas fracture, the next major fracture zone to the south. Moving southerly, normal to the fracture zones along about 235°, each offset brings successively younger plate further west. The eastern portion of this Line Islands anomaly is probably the result of this cummulative effect in offset. This anomaly also diminishes westward and then increases again, suggesting a change in the age of offset, which along the Galapagos fracture zone may even change sign (Pitman et al., 1974).

Pitcairn anomaly is the only one of these positive anomalies that is bounded by the east Pacific rise itself. It is bounded by the Marquesas fracture zone on the north and the Challenger on the south. The offset in age across these fracture zones is largest nearer the ridge and decreases westward. This has the effect of producing an anomaly nearer the ridge that attenuates rapidly to the west. The anomaly itself lies almost wholly on sea floor formed upon reorganization of the east Pacific rise beginning about 60 m.y.b.p. (Herron, 1972). At this time the northwesterly trending ridge migrated north of the Eltanin fracture zone forming a new, northeast trending ridge and reorienting fracture zones to strike west-northwest. These newer fracture zones and young lithosphere produce the Pitcairn anomaly.

Although these interpretations in light of the presence of fracture zones having significant offsets in age seem reasonable, they are only qualitative. But they can be put on a firmer basis by computing a synthetic geoid based strictly on the relative ages of the Pacific plate; which is now in progress (Marsh and Hinojosa, 1983). This is quite feasible for the Pacific plate because of the relative paucity of voluminous off-ridge volcanism for large distances near the west flank of the east Pacific rise.

Possible Size and Ascent Velocity of Hot Spot Plumes

Although the surficial expression of hot spots as volcanism and their kinematic implications are by now clearly evident, there is much less certainty about their subsurface structure and ultimate origin. That is little is known of the fluid mechanical conditions within the mantle that gives rise to these features. Morgan (1971, 1973) has suggested that they originate deep within the lower mantle as buoyant plumes, perhaps emanating from the region of the core-mantle boundary itself. Judging from the wide nature of lithospheric swells (≈1000 km), and using a "simple aspect-ratio arguement", Crough (1978) has also suggested that these plumes originate from the lower mantle or at the core-mantle boundary itself. Sandwell (1982) has attempted to place bounds on the diameter of the hot-spot below the lithosphere by computing the gravity, geoid, topography, heat flow, and subsurface temperature as a function of diameter and plate velocity using an imposed temperature distribution. These results are not particularly diagnostic, but they suggest a sub-lithospheric hot-spot diameter of 400-4000 km. It is the intent of this section to show some additional relationships between plume size, mantle viscosity, and heat transfer during ascent.

A necessary assumption in relating hot-spots to a source region for plumes is that the plume must travel fast enough to the earth's upper most regions without cooling and loosing its buoyancy. The rate of cooling depends critically on the diameter of the plume which is controlled by the viscosity field in the source region. Plumes rise as a result of a density inversion or gravitational instability. It has been shown through analysis and experiment that the characteristic size (a = radius) of a plume (of viscosity μ_2) emanating from such a low density layer (of viscosity μ_1) is given by (Marsh, 1979)

$$a \approx \frac{h_2}{2}\left(\frac{\mu_1}{\mu_2}\right)^{1/4} \qquad (4)$$

where h_2 is the initial thickness of the source layer. If $\mu_1 \approx \mu_2$, the plume has a diameter about equal to the thickness of its source layer, which is approximately observed for salt domes within the earth's crust.

A buoyant layer within the mantle could be produced by anomalous heating. The viscosity, which is otherwise nearly uniform (Cathles, 1973), could also be lowered by this heating. The reduction in viscosity, however, is unlikely to be by more than a factor of 100 (poise) (e.g. Marsh, 1982) unless it is partially melted, but there is no evidence that the temperature of the deep mantle is near its solidus. From Figure 5, computed from (4), for $\mu_1/\mu_2 \approx 100$ the plume diameter is about three times the thickness of its source layer. Since a source layer much thicker than about 100 km would be readily detectable by seismic methods, the plume diameter would be about 300 km; even for a viscosity contrast of 10^4, the diameter is only about 400 km. The main lesson of equation (4) is that the plume diameter will be of the same order as the thickness of its source.

Unless the source layer thickness is greater than about 5-10 times its depth, there are no results associated with the fluid mechanics of gravitational instabilities that give any information on the actual depth of the source (Marsh, 1975). The only region within the mantle where it is dynamically reasonable to suspect plume growth is within hot thermal boundary layers. Such a layer may occur at the core-mantle boundary (Elsasser et al., 1978), which may be associated with the D" seismic layer,

although this is controversial. If the mantle has two or more tiers of convection cells, hot thermal boundary layers could also occur within the body of the mantle itself, but their existence is highly controversial.

A small plume ascending from great depth may cool and loose its buoyancy before reaching the base of the lithosphere. Its final temperature depends critically on its rate of ascent, and even a small plume ascending sufficiently fast will hardly cool at all. This relationship between ascent velocity, final temperature, and plume velocity may be investigated through a model of heat transfer. These models and methods have been extensively developed by Marsh (1978; 1982) and Marsh and Kantha (1978), for understanding the heat transfer of ascending bodies of magma. The method is parametric and general and may be used for any geometry, and only a brief description is given here.

By conservation of energy, the mean temperature (T) in a plume changes with time in response to the total flux of heat (Q_T) from the body and that due to adiabatic decompression ($-\gamma T$).

$$\rho C_p V' \frac{dT}{dt} = -Q_T - \gamma(T) / \rho C_p V' \qquad (5)$$

where ρ is density, C_p is specific heat, V' is volume and γ is the usual adiabatic coefficient; all of which are considered constant (although this is not a necessary assumption). A dimensionless number involving Q_T can be conveniently defined as

$$Nu = \frac{Q_T}{Q_{cd}} \qquad (6)$$

where Nu is the well known Nusselt number, a pure number, and Q_{cd} is the heat flux due to conduction (i.e. when the body is motionless). The flux

$Q_{cd} = AKc(T-T_m(t))/L$, where A is the surface area involved in the heat transfer, Kc is thermal conductivity, $T_m(t)$ is the characteristic mantle geotherm far from the plume, and L is the characteristic length scale of heat conduction; for a plume L = radius (a). Substituting Q_{cd} and (6) into (5) and rearranging gives (Marsh, 1978)

$$\frac{dT}{dt} + JT = JT_m(t) - \gamma T \tag{7}$$

where $J = Nu(AKc)/(L\rho CpV')$. This has the general solution

$$T = Je^{-J't} \int T_m(t)e^{J't}\,dt \tag{8}$$

where $J' = J + \gamma$, when coupled with an intial condition this describes the mean temperature of the body as a function of time or distance from its source. Since the final temperature must be greater then $T_m(L)$, where L is the total ascent distance, this places a condition on the ascent velocity. Although the ascent velocity has not yet appeared explicitly, it enters through the relationship for Jt.

For magmatic transfer through the lithosphere, solutions to (8) are given by Marsh (1978; 1982) and Marsh and Kantha (1978) where transfer by diapirism, stoping, zone melting, and pipe flow are considered. Here we consider an anomalous hot plume ascending from a buoyant region. The region itself need not be globally continuous , but only locally continuous. Its mean temperature is Tp, which is the temperature of the plume itself at its source. The normal mantle temperature at this depth is T_o.

The mantle temperature is taken to be adiabatic throughout the mantle, and hence varies as $T_m(t)/T_o = EXP(-\gamma t)$ with depth (or time) until near the uppermost mantle. Substituting $T_m(t)$ into (8) gives upon integration

$$\frac{T}{T_o} = EXP(-(\gamma t_o)t') - EXP(-((J+\gamma)t_o)t') + (T_p/t_o)EXP(-((J+\gamma)t_o)t') \qquad (9)$$

where the intial condition T(0) = Tp has been used. The mean temperature of the plume as a function of $t'(= t/t_o)$ and Jt_o as described by (9) is given by Figure 6. Both the mantle and the plume have been assumed to have the same adiabatic coefficient ($\gamma = \alpha g t_o/Cp = 0.7$, where Cp is specific heat and other symbols as before).

The results of Figure 6 suggest that if the plume is to remain hot and buoyant and reach the upper mantle $Jt_o \approx 1$, from which the ascent velocity can be calculated. Recalling that $J \equiv (NuAKc)/(L\rho CpV')$, where for a plume $A/V' = 2\pi a\ell/\pi a^2\ell = 2/a$, where a is radius and ℓ is a length, $Kc/\rho Cp \approx 10^{-2} cm^2/s$, and L = a, we have $J = Nu2x10^{-2}/a^2$. It is clear that Nu must now be used and several choices are possible. The Nu for a plume can be approximated by that for flow in a pipe, which for a fully developed pipe flow is well known to be 4.36 (e.g. Kays, 1966). This result holds only far from the thermal entry region of the pipe. The length of the thermal entry region for most geophysical flows is large (Marsh, 1978) and it is proportional to Va^2/K, where V is velocity. If $V \approx 10^{-7}$cm/s, $a \approx 10^7$cm and $K \approx 10^{-2} cm^2/s$, the thermal entry length is about 10^4 km, and for larger velocities it increases. Thus Nu = 4.36 is a conservative approxiamtion for heat transfer, more than likely it will be significantly larger, even by a factor of ten.

Then, $J = 8.72 \times 10^{-2}/a^2$ and the total ascent time is given by $t_o = 115Ha^2$, where H is the numerical value of Jt_o from the curves of Figure 6.

For $Jt_o = 1 = H$ and, from Figure 5 for, say, $a = 200$ km, the ascent time is $t_o = 4 \times 10^{15}$ sec, which for an ascent distance of 2500 km, gives a typical ascent velocity of about 2 cm/yr. That is, if a plume of a diameter of 400 km ascends a distance of 2500 km at a velocity of about 2 cm/yr, it will still be anomalously hot when it arrives in the upper mantle. It must be reminded, however, that this is an absolute mimimum velocity. For a more reasonable Nu (≈10x larger) the velocity must be 20 cm/yr, and if the radius is 100 km, V ≈80 cm/yr. The main result of this calculation is that it is apparently possible even for relatively small plumes to ascend a large distance through the mantle without totally loosing their original anomalous temperature. It should also be pointed out, however, that even an adiabatic plume cools more than an equivalent "normal" mantle during its ascent. This is because the adiabatic temperature change is proportional to the temperature of the body itself. Hence even for identical thermal properties, a hotter body cools faster than an equivalent cooler body.

Conclusions

The gravity field over the Pacific determined by Sjogren's method with about 90 passes of GEOS-3/ATS-6 satellite-to-satellite tracking data. This new determination is in good agreement with our previous (1981) determination of the gravity field in this area using 40 passes of SST data. A comparison of this map with the more conventially-determined GEM satellite gravity field

shows good agreement. We also show the geoid over the Pacific determined from SEASAT altimeter data and it too agrees well with both GEM and SST, but this geoid contains far more detail than either of these other maps.

It has been previously noted that areas with residual depth anomalies associated with hot-spots correlate with geoid and gravity anomalies. These so-called swells do often correlate with the present maps, but there are some clear exceptions and complications. The Marquesas-Line swell of Crough and Jarrard (1981) was found by them to correlate well with the GEOS-3 geoid of Brace (1977). The positive geoid anomaly near the Marquesas Islands of that work, however, was not found in our earlier SST study (Marsh et al., 1981) and the present fields verify its absence. This errant positive anomaly is apparently the result of poor GEOS-3 coverage in this area.

Those anomalies not associated with thermal swells correlate well with relatively young areas of the seafloor bounded by fracture zones. Because the major fracture zones of the Pacific are fairly evenly spaced and trend approximately east-west, they produce a similar fabric in the gravity and geoid fields. The anomalies are essentially framed by these fracture zones. For a typical offset in age of ≈15 m.y. the resulting geoid anomaly is about 2.5 m, which is close to that observed near the east Pacific rise. Because the traces of hot spots are not parallel to fracture zones, there is an interference in anomalies from each source. The resulting anomaly field may thus be separable using the known ages and history of the Pacific plate. Early modeling shows that because the anomalies due to age offsets attenuate with absolute age, large geoid anomalies over older sea floor (∿70 m.y. like NE of Hawaii) can not be completely explained by this offset alone (Marsh and Hinojosa, 1983). A part of the cause may also be below the lithosphere.

An examination of the size and ascent velocity necessary to bring mantle plumes to the upper mantle without cooling shows that plume diameter is apt to be of the same order as the thickness of its source. Because low density regions within the mantle thicker than about 1000 km, were they to exist, should have been discovered through seismology, plume diameter is probably limited to less than about 400 km. And the ascent velocity needed to prevent complete cooling is at least 3 cm/yr; it could be ten times larger.

The explanation of this distinctive pattern of gravity and geoid anomalies in the Pacific has been of interest since the first indication of its presence (Marsh and Marsh, 1976). At that time we suggested they might reflect the presence of a small scale form of convection in the uppermost mantle. Because several of these anomalies begin very near the east Pacific rise and because some time is necessary to initiate small scale convective rolls, McKenzie et al. (1980) suggested that these anomalies must arise from small scale convective instabilities in the lower limb of a larger cell confined to the upper mantle. These secondary instabilities would then be already established as they reached the ridge itself. The close correlation between sea-floor age, fracture zones and these near-ridge anomalies makes the interpretation of McKenzie et al. (1980) untenable. In fact as it now appears the structure of the lithosphere itself may be a major factor in causing these distinctive anomalies. Nevertheless, the ultimate origin of both hot spots, the regularity of fracture zones with major offsets, and some geoid anomalies over old, smooth sea floor is still unknown, and they could conceivably be related to the effects of small convection.

Acknowledgements

B.M. thanks Ray Arvidson for an early image-analysis of the Pacific bathymetry. This work is supported by a grant (NAG5-32) to the Johns Hopkins University from the National Aeronautics and Space Administration.

References

Brace, K. L., 1977, Preliminary ocean-area geoid from GEOS-3 satellite radar altimetry. St. Louis Air Force Station, Nov. 1977.

Cathles, L. M., III, The viscosity of the Earth's mantle. Princeton Univ. Press, 389 p., 1975.

Cochran, J. R. and M. Talwani, Free-air gravity anomalies in the world's oceans and their relationship to the residual elevation. Geophys. J. R. Astr. Soc.,v.50, p. 495-552, 1977.

Crough, S. T. and R. D. Jarrard, The Marquesas-Line swell. Jour. Geophys. Res., 86, 11763-11771, 1981.

Crough, S. T., Thermal origin of mid-plate hot spot swells. Geophys. Jour. R. Astronom. Soc., 55, p. 45-469, 1978.

Detrick, R. S., Jr., An analysis of geoid anomalies across the Mendocino fracture zone: Implications for thermal models of the lithosphere. Jour. Geophys. Res., 86, 11,751-11,762, 1981.

Duncan, R. A. and I. McDougall, Migration of volcanism with time in the Marquesas Islands, French Polynesia. Earth and Plant. Sci. Letts., 21, 414-420, 1974.

Elsasser, W. M., P. L. Olson, and B. D. Marsh, The depth of mantle convection. Jour. Geophys. Res., 84, 147-155, 1979.

Haxby, W. F. and D. L. Turcotte, On Isostatic Geoid Anomalies. J. Geophys. Res., 83, p. 5473-5478, 1978.

Herron, E. M., Sea floor spreading and the Cenozoic history of the east-central Pacific. Geol. Soc. Amer. Bull., 83, 167-1692, 1972.

Lerch, F. J., C. A. Wagner, S. M. Klosko, R. P. Belott, R. E. Laubscher, and W. A. Taylor, Gravity model improvement using GEOS-3 altimetry (GEM-10A and 10B). J. Mar. Geod, (in press).

Lerch, F. J., J. G. Marsh, S. M. Klosko, and R. G. Williamson, Gravity model improvement for SEASAT. Jour. Geophys. Res., 87, 3281-3296, 1982.

Marsh, B. D., Plume spacing and source. Nature, 256, 240, 1975

Marsh, B. D., On the cooling of ascending andesitic magma. Phil. Trans. Roy. Soc. London. A., 288, 611-625, 1978.

Marsh, B. D., Island Arc Development: Some observations, experiments, and speculations. Jour. Geol., 87, 687-713, 1979.

Marsh, B. D., On the mechanics of igneous diapirism, stoping, and zone melting. Amer. Jour. Sci., 282, 808-855, 1982.

Marsh, B. D., Kantha, L. H., On the heat and mass transfer from an ascending magma. Earth and Planetary Sci. Letts., 39, 435-443, 1978.

Marsh, B., and J. Hinojosa, 1983,SEASAT Geoid Anomalies in the Pacific: Two Dimensional Spectra and Removal of Plate Sources (abstract). AGU Spring Meeting '83.

Marsh, B. D. and J. G. Marsh, On Global gravity anomalies and two-scale mantle convection. Jour. Geophys. Res., 81, 5267-5280.

Marsh, J. G., B. D. Marsh, R. G. Williamson, and W. T. Wells, The gravity field in the central Pacific from satellite-to-satellite tracking. Jour. Geophys. Res., 86, p. 3979-3997, 1981.

Marsh, J. G. and T. V. Martin, The SEASAT altimeter mean sea surface model. Jour. Geophys. Res., 87, 3269-3280, 1982.

McKenzie, D., A. Watts, B. Parsons, and M. Roufosse, Planform of mantle convection beneath the Pacific Ocean. Nature, v. 288, p. 442-446, 1980.

Morgan, W. J., Convection plumes in the lower mantle. Nature, v. 230, p. 42-43, 1971.

Morgan, W. J., Plate motions and deep mantle convection. Geol. Soc. Amer. Mem., 132, 7-22, 1972.

Nemoto, K., and L. W. Kroenke, Marine geology of the Hess Rise I. Bathymetry, surface sediment distribution, and environment of deposition. J. Geophys. Res., 86, 10,734-10,752, 1981.

Parsons, B., and J. G. Sclater, An analysis of the variation of ocean floor bathymetry and heat flow with age. Jour. Geophys. Res., 82, 803-827, 1977.

Pitman, W. C., III, R. L. Larson, and E. M, Herron, Magnetic lineations of the oceans. Geol. Soc. Amer, Map. 1974.

Sandwell, D. T., Thermal isostasy: Response of a moving lithosphere to a distributed heat source. J. Geophys. Res., 87, 1001-1014, 1982.

Sandwell, D. T. and G. Schubert, Geoid height versus age for symmetric spreading ridges. J. Geophys. Res., 85, 7235-7241, 1980.

Sandwell, D. T. and G. Schubert, Geoid height-age relation from SEASAT altimeter profiles across the Mendocino fracture zone. Jour. Geophys. Res., 87, 3949-3958, 1982.

Tapley, B. D., G. H. Born, M. E. Parke, The SEASAT altimeter data and its accuracy assessment. Jour. Geophys. Res., 87, 3179-3188, 1982.

Turcotte, D. L. and D. C. McAdoo, Geoid anomalies and the thickness of the lithosphere. J. Geophys. Res., v. 84, p. 2381-2387, 1979.

Turner, D. L. and R. D. Jarrard, K-Ar dating of the Cook-Austral island chain: A test of the hot-spot hypothesis. J. Volcanology and Geothermal Res., 12, 187-220, 1982.

Watts, A. B., Gravity and Bathymetry in the central Pacific Ocean, J. Geophys. Res., v. 81, p. 1533-1553, 1976.

Watts, A. B., J. H. Bodine, and N. M. Ribe, Observations of flexure and the geological evolution of the Pacific Ocean basin. Nature, 283, 532-537, 1980.

Figure Captions

Figure 1. Distribution of SST tracks used in this study.

Figure 2. SST gravity map for the central Pacific region. The circles have radii of 30° and 40° about the subsatellite point, and within this range the gravity is essential radial.

Figure 3. SEASAT altimeter geoid for the Pacific relative to the twelfth degree and order GEM 10B geoid. The trace of the east Pacific rise is also shown (far right) as well as the 20 and 65 m.y. isochrons for the age of the Pacific plate.

Figure 4. The SEASAT geoid of Figure 3 superimposed on the map of the age of the ocean basins of Pitman et al., (1974).

Figure 5. The relationship between the diameter (2a) of a plume rising from a low density region of thickness h_2 and viscosity μ_2 relative to a surrounding mantle of viscosity μ_1. The right axis gives diameter for a source thickness of 100 km.

Figure 6. The mean temperature (T/T_o) of a section of plume as it ascends through mantle whose temperature is adiabatic and described by Tm(t). Only for values of $Jt_o \approx 1$ does the plume reach the upper mantle still anomalously hot.

GEOS-3/ATS-6 SATELLITE TO SATELLITE GROUND TRACKS

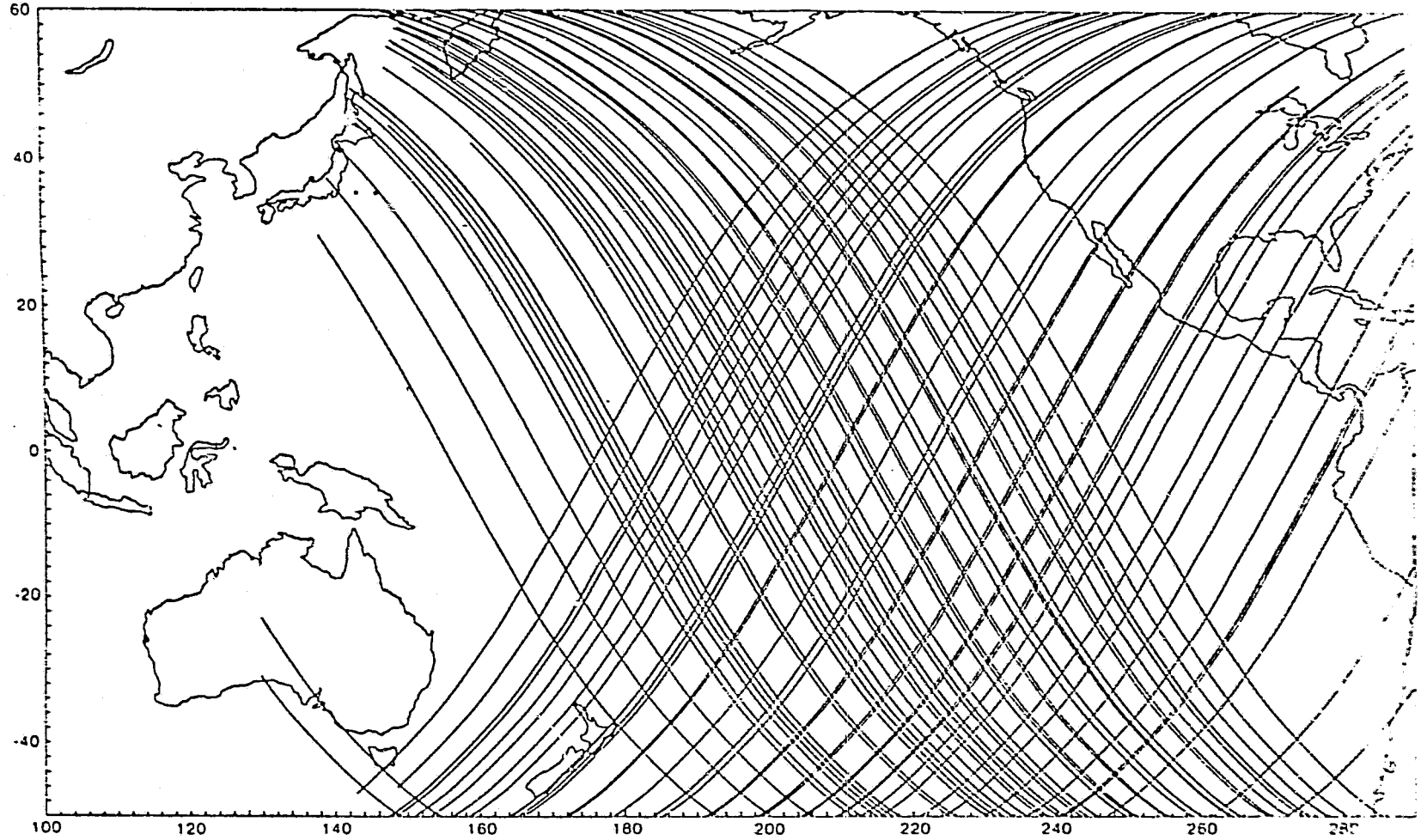

Figure 1. Distribution of SST tracks used in this study.

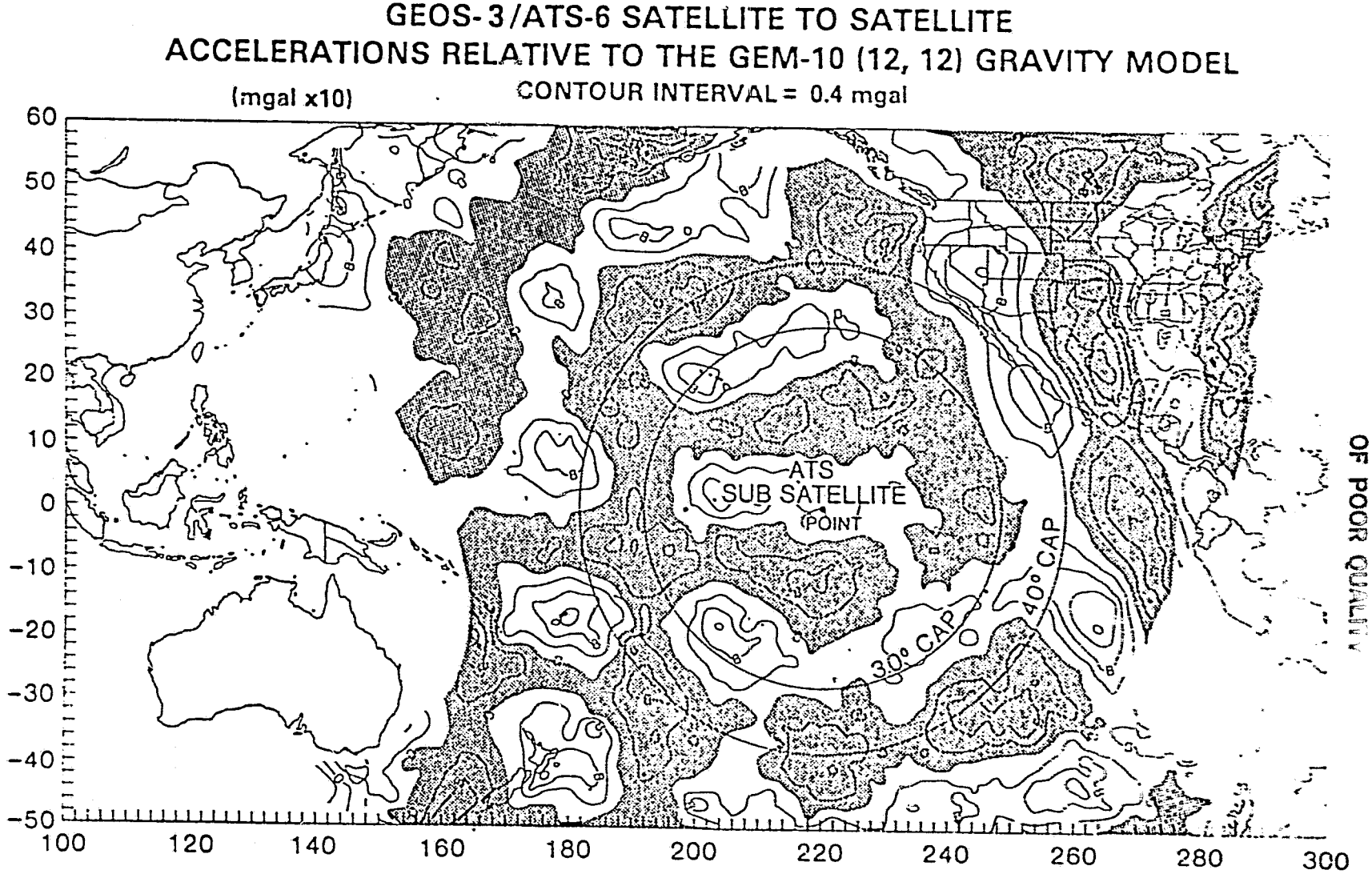

Figure 2. SST gravity map for the central Pacific region. The circles have radii of 30° and 40° about the subsatellite point, and within this range the gravity is essential radial.

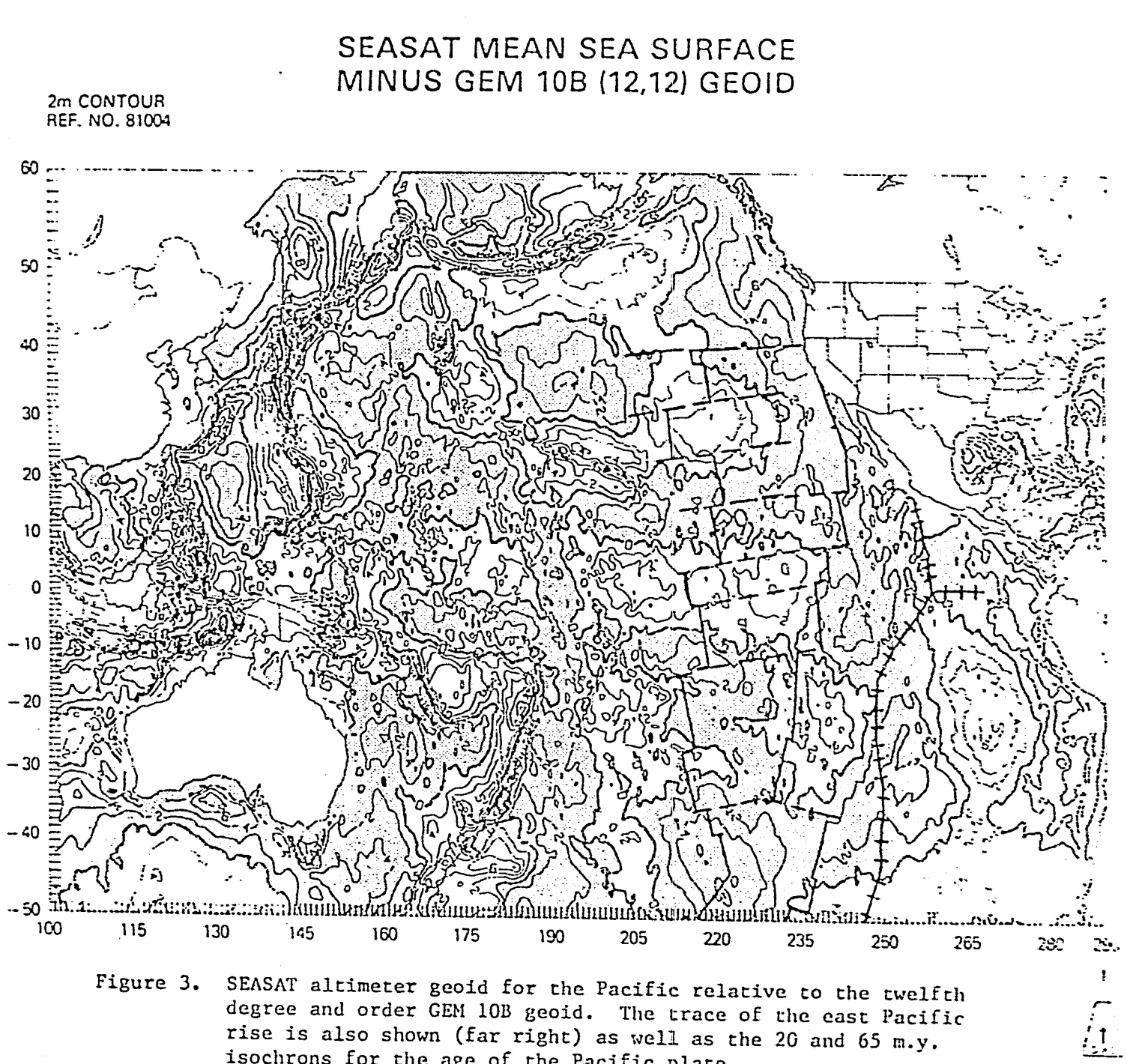

Figure 3. SEASAT altimeter geoid for the Pacific relative to the twelfth degree and order GEM 10B geoid. The trace of the east Pacific rise is also shown (far right) as well as the 20 and 65 m.y. isochrons for the age of the Pacific plate.

SEASAT GEOID MINUS GEM 10B 12,12
OVER AGE OF OCEAN FLOOR

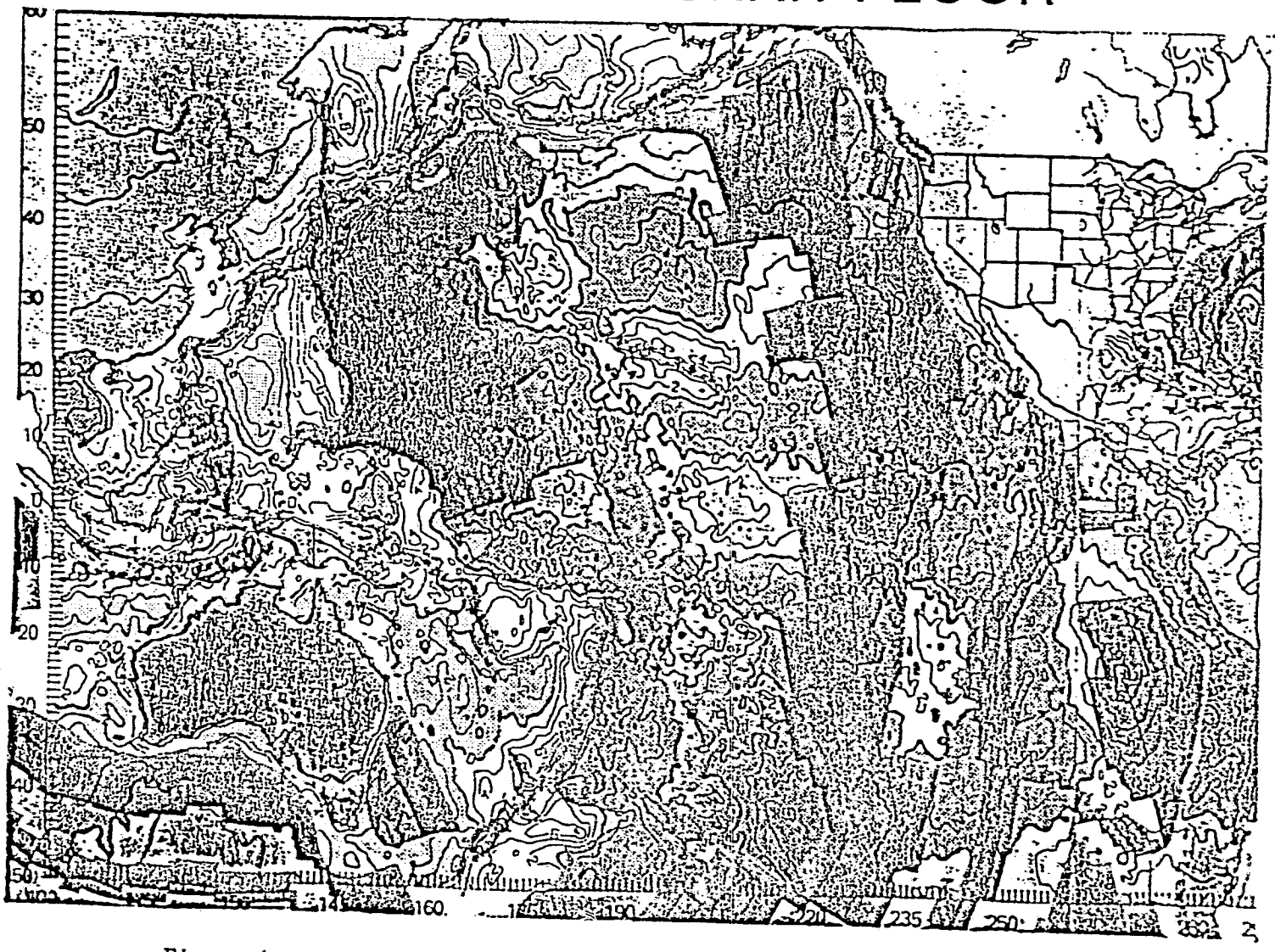

Figure 4. The SEASAT geoid of Figure 3 superimposed on the map of the age of the ocean basins of Pitman et al., (1974).

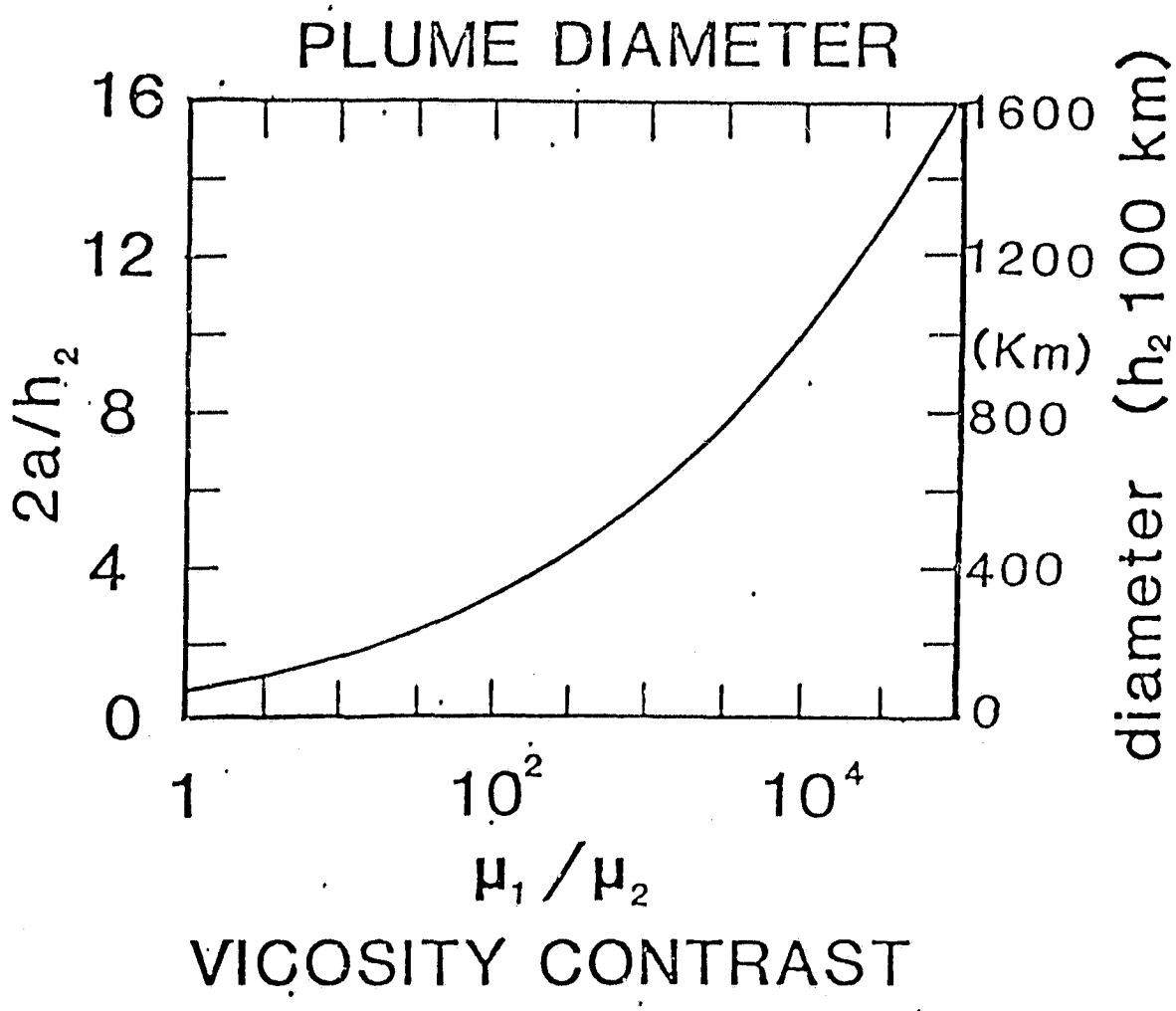

Figure 5. The relationship between the diameter (2a) of a plume rising from a low density region of thickness h_2 and viscosity μ_2 relative to a sourrounding mantle of viscosity μ_1. The right axis gives diameter for a source thickness of 100 km.

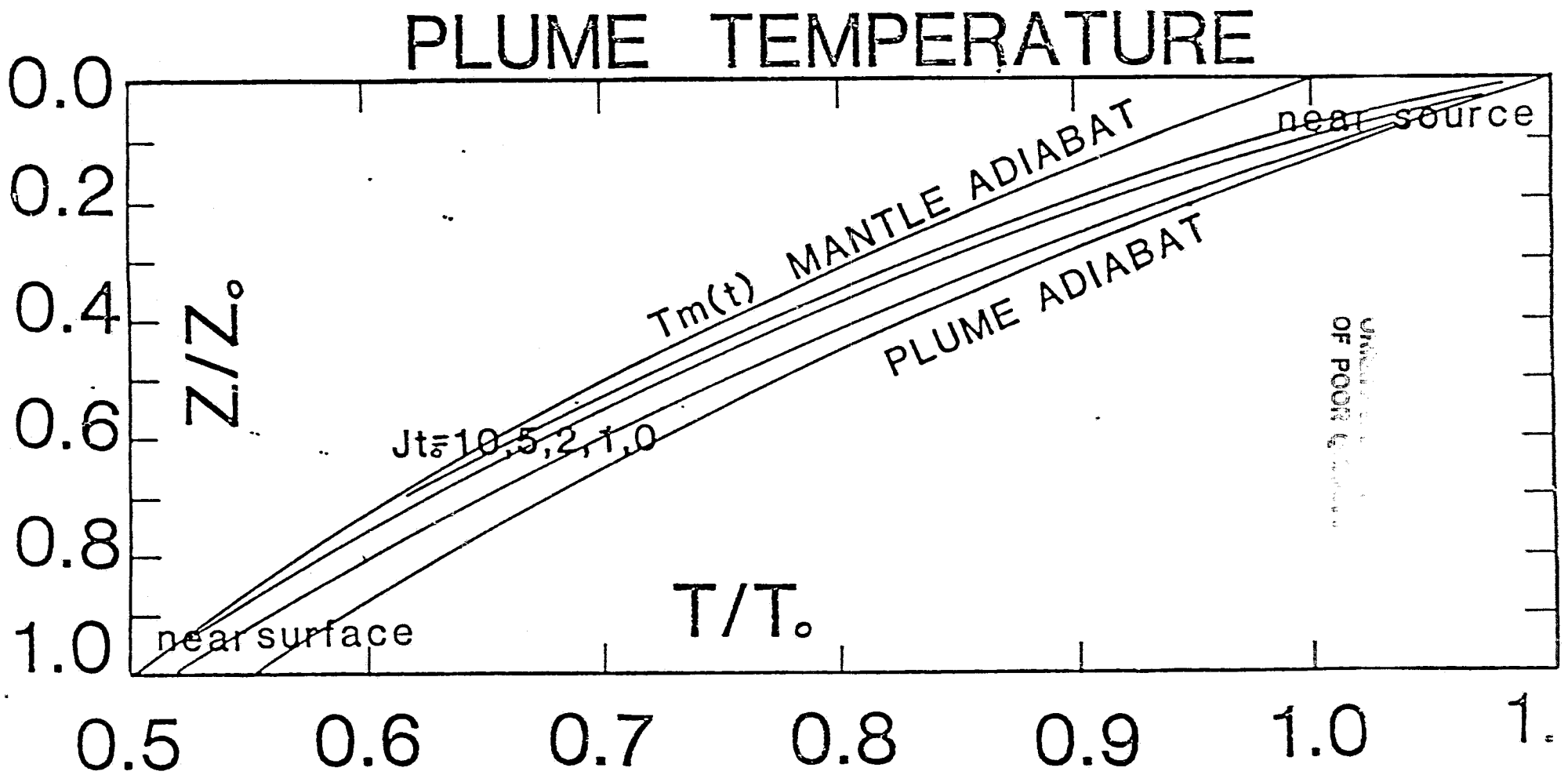

Figure 6. The mean temperature (T/T_o) of a section of plume as it ascends through mantle whose temperature is adiabatic and described by Tm(t). Only for values of $Jt_o = 1$ does the plume reach the upper mantle still anomalously hot.